PHYSICAL REVIEW B VOLUME 10, NUMBER 8 15 OCTOBER 1974

Band inversion and transport properties of L minima in n-GaSb(Te)†

Ru-Yih Sun and W. M. Becker
Department of Physics, Purdue University, West Lafayette, Indiana 47907
(Received 22 April 1974)

Electrical transport measurements have been made on tellurium-doped n-type GaSb in the temperature range between 1.4 to 300 °K and at hydrostatic pressures up to $\sim$ 13 kbar. Samples with concentration in the range $\sim 2\times 10^{17}$ to $\sim 7\times 10^{18}$ cm^{-3} were investigated. At the highest pressures, the results suggest complete carrier transfer from the Γ minimum into the L minima or into impurity levels associated with the L minima. The existence of the levels is confirmed by the observation of impurity conduction at low temperatures and deionization effects at elevated temperatures. An impurity activation energy of $\epsilon_1 = 13.8$ meV is seen for the tellurium donors in the lowest-concentration sample; the activation energy decreases with incréasing concentration but remains nonzero in the highest-concentration sample. Weak-field magnetoresistance anisotropy was observed, and the relations $b+c=0$ and $d>0$ for the inverted Seitz coefficients were found to hold at high pressures in the temperature range where L-band conduction is expected. Calculations indicate that in highly doped samples, acoustic mode scattering dominates at 300 °K, whereas at 77 °K the L-band carrier scattering is mainly due to ionized impurities. The results obtained for pressures insufficient to produce complete thermal decoupling between the Γ minimum and the Te levels associated with the L minima are shown to be predictable using a band model employed by Kosicki and Paul.

I. INTRODUCTION

In recent years, intensive investigations have been carried out on semiconductors in which the impurities give rise to states associated with higher-lying-conduction-band minima; these minima have symmetries different from the lowest-lying conduction band. In some cases, these states lie below the lowest-conduction-band edge and can be easily demonstrated experimentally. In other cases, such impurity states lie above the conduction-band edge and are said to be "resonant" with the band states of the deeper minimum; such states are difficult to study experimentally.[1–4] The same impurities also give rise to bound states associated with the lowest conduction band.

One approach to the study of resonance states has been to apply hydrostatic pressure and thus induce a shift of the band minima sufficient to convert the resonance states to bound states.[5] In the material of interest here, the III-V semiconductor, GaSb, band crossing between the lowest-lying conduction band (Γ) and the next higher band (L) can be accomplished at pressures of ~10 kbar, and pressure studies have been utilized in this material to investigate the resonance states introduced by Te donors. A survey of the literature indicates that in pressure measurements of the transport properties of n-GaSb(Te), these investigations are predominantly confined to resistivity measurements at fixed temperature.[5–10] In the results to be reported here, we examine the pressure dependence of the galvanomagnetic properties of n-GaSb(Te) as a function of temperature. Our work represents the first systematic investigation of these properties over the complete concentration range available for this material.

In a preliminary communication,[11] we reported the observation of activation energies associated both with impurity conduction and with L-band impurity states. This earlier work was confined to a discussion of a single low-concentration sample, and utilized resistivity and Hall-coefficient data. In the present work, we give systematic details relating to changes in impurity activation energy with concentration for a wide range of impurity concentrations (10^{17}–$\sim 10^{19}$ cm^3). In addition to resistivity and Hall-effect results, we also present magnetoresistance data establishing the anisotropy parameters of the L-conduction-band minima; this represents the first measurement of these parameters in GaSb which precludes effects due to the presence of Γ-band carriers. Finally, the limitations of the high-pressure technique used in our work are discussed as part of the evaluation of the data.

II. EXPERIMENTAL

Hydrostatic-pressure measurements were carried out in a Cu-Be bomb using a 50% mixture of kerosene and mineral oil as the pressure-transmitting medium. The bomb is closed and pressurized at room temperature. Pressures are measured with a manganin gauge. Cooling of the bomb to ~150 °K results in a ~3-kbar decrease in pressure; no further changes in pressure are expected at lower temperatures.[12] Above pressures $P > P_s$ apparently sufficient to produce complete carrier transfer out of the Γ minimum, the galvanomagnetic properties become independent of pressure

over the temperature range ~(77–300)°K. For $P \leq P_s$, the results are complicated by the pressure changes which occur in the bomb for $T \gtrsim 150$ °K because of differential thermal expansion between the bomb and the pressure-transmitting medium. A chromel versus Au–0.07-at.%-Fe thermocouple was attached to the wall of the bomb to monitor the sample temperature. Analysis of sample data indicated that there was no thermal lag between the temperature of the sample and the temperature of the outer wall of the bomb for the procedures employed in the measurements. In the lowest-concentration samples, heating of the sample occurred when using conventional dc techniques. In these few cases, galvanomagnetic measurements were carried out using pulsed electric field techniques; the fields employed were limited to the Ohmic region. Hall plates were cut perpendicular to the growth axis to reduce inhomogenity. The orientation was established by x-ray analysis. Typical sample sizes were $8 \times 1 \times 1$ mm^3. Two current and four potential contacts were applied using cerroseal 35 solder. The sample homogeneity observed at $P=0$ was maintained throughout the various pressure and temperature cycles employed in acquiring the data, indicating that significant shear and inhomogeneous strains are not supported by the pressure-transmitting medium.

III. RESULTS

A. $\rho(T)$ and $R_H(T)$ as a function of pressure

At low pressures, the temperature dependence of the transport properties in low-concentration samples is expected to be relatively independent of pressure. With increasing pressure, carrier-

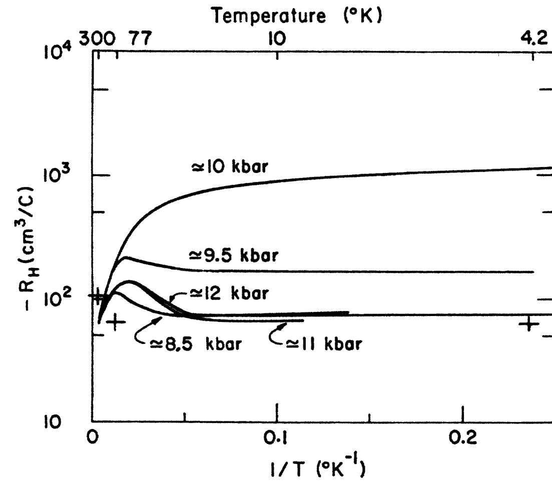

FIG. 2. Hall coefficient R_H vs reciprocal temperature for sample 97CT [R_H(4.2 °K, $P=0$) = −65 cm^3/C]. +, $P=0$ (1 atm). All pressures noted on graph measured at 300 °K. Data points deleted for sake of clarity.

transfer effects should become detectable. Figures 1–3 give the behavior of the low-concentration sample 97 CT for $8.5 \leq P$ (300 °K) ≤ 12.0 kbar, as well as data points for $P=0$. The zero-pressure results are consistent with published data,[6,13] and have previously been interpreted in terms of a temperature-dependent distribution of carriers between the Γ and L conduction-band minima. Allgaier[14] has noted that the condition necessary for a Hall maximum to be seen for a model of two conduction bands and band edges separated in energy by ΔE is $bP > 1$, where $b = \mu_2/\mu_1$ and $P = (\nu_2/\nu_1)(m_2^*/m_1^*)^{3/2}$. (In Allgaier's analysis ν_i and m_i denote the number of

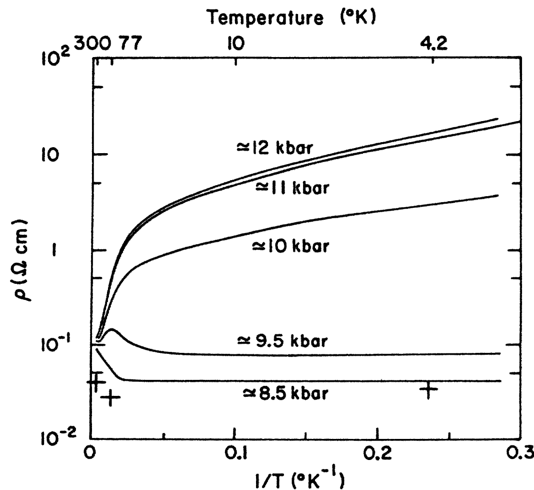

FIG. 1. Resistivity ρ vs reciprocal temperature for sample 97CT [R_H(4.2 °K, $P=0$) = −65 cm^3/C]. +, $P=0$ (1 atm). All pressures noted on graph measured at 300 °K. Data points deleted for sake of clarity.

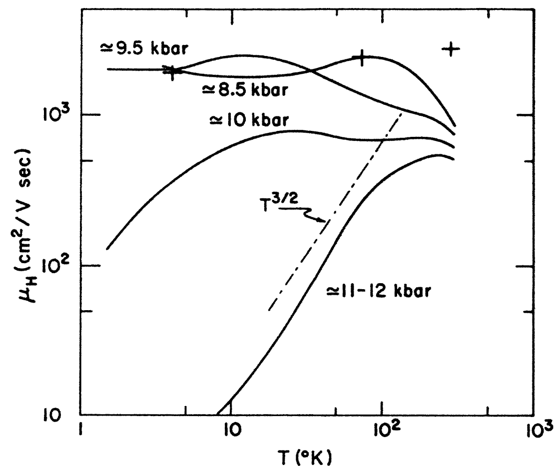

FIG. 3. Hall mobility μ_H vs temperature for sample 97CT [R_H(4.2 °K, $P=0$) = −65 cm^3/C]. +, $P=0$ (1 atm). All pressures noted on graph measured at 300 °K. Data points deleted for sake of clarity. Dash-dot line, μ_H (L-band carriers) assuming ionized impurity scattering only.

valleys and density-of-states effective mass of each band, respectively; the band subscripts are in the order of increasing energy. For the case of GaSb, $\nu_1 = \nu_\Gamma = 1$ for the Γ band, and $\nu_2 = \nu_L = 4$ for the L band.) This condition is satisfied in low-concentration n-GaSb(Te), but the Hall maximum is expected at a temperature greater than 300 °K at zero pressure. However, in Fig. 2 a maximum in R_H is clearly observable below room temperature for P (300 °K) $\cong 8.5$ kbar; this maximum is ascribed to the temperature-induced transfer of carriers between the Γ and L bands as ΔE becomes small. SdH results have indicated that the 4.2 °K, $P=0$ Hall coefficients for low-concentration samples of n-GaSb(Te) are to within a few percent a direct measure of the concentration of the carriers in the Γ minimum.[15] Assuming R_H ($T=4.2$ °K, $P=0$) is the low-temperature limit R_L for $P=8.5$ kbar as defined by Allgaier, then

$$R_{max}/R_L = (1+b)^2/4b \,. \quad (1)$$

The ratio $R_{max}/R_L = 1.8$ is estimated from the data given in Table I and in Fig. 2 for sample 97 CT. Therefore $b = \mu_2/\mu_1 = \mu_L/\mu_\Gamma \simeq \frac{1}{5}$, which is the range of generally accepted values for this parameter in low-concentration samples. Also, as seen in Fig. 3, $\mu_\Gamma \sim 2500$ cm^2/V sec and is fairly independent of temperature at $P=0$. The higher-pressure data indicates that $\mu_L \sim 500$ cm^2/V sec down to ~150 °K, where the Hall maximum is observed. Thus the ratio μ_L/μ_Γ derived from the Hall data is also consistent with the separate mobility results given in Fig. 3.

For the Hall-effect behavior under discussion [P (300 °K) ~ 8.5 kbar], the pressure at 4.2 °K is ~5.5 kbar. Assuming a Γ-L closing rate of $\partial\Delta E/\partial P = -10$ meV/kbar,[5,7,9] the Fermi level at 4.2 °K is expected to be 20 ± 3 meV below the L-band edge. An observed increase of the Hall coefficient over the zero-pressure value at 4.2 °K suggests that depopulation from the Γ band into low mobility states takes place at pressures below those required for carrier transfer into the L band. Both L-band tail states as well as localized Te impurity states associated with the L-minima have been invoked to explain similar results.[9,16,17] We will show from our data that the carrier transfer is into discrete states or into a narrow band which is well below the L-band edge.

With further increase in pressure, the Hall maximum moves toward lower temperatures. In this intermediate pressure range, conduction in both the Γ and L bands must be considered at high temperatures, whereas at low temperatures, impurity conduction and transport by Γ-band carriers dominate. At the highest pressures, the high-temperature conduction is by the L-band carriers and a Hall maximum reappears as a consequence of a temperature-dependent distribution of carriers between the L band and lower-lying conducting states introduced by the Te donors.

At $P \lesssim P_s$, the appearance of a distinct region of temperature activation in the resistivity at high temperatures suggests that carriers are being ionized from Te states into the L band. As seen in Fig. 1, the apparent activation energy is a function of pressure. Analysis of the high-temperature behavior is complicated by factors such as (i) changes in ΔE due to pressure changes in the closed bomb, (ii) the temperature dependence of ΔE, and (iii) changes in mobility of the L-band carriers with change in Fermi energy. Since the magnitudes of these effects are not well known, we first experimentally establish a pressure region above which no further changes in the high-temperature resistivity or Hall effect are observed. As seen in Figs. 1–3, this result occurs at P (300 °K) ≥ 11 kbar in sample 97CT.

TABLE I. Sample Hall coefficient, resistivity, and Hall-mobility values at $T=4.2$ °K and atmospheric pressure ($P=0$).

Sample	R_H (cm^3/C)	ρ (Ω cm)	μ_H (cm^2/V sec)
96AT	−70.5	4.55×10^{-2}	1.55×10^{3}
97CT	−65.0	3.49×10^{-2}	1.86×10^{3}
96Am I[a]	−30.4	8.05×10^{-3}	3.78×10^{3}
96AM II	−25.6	6.84×10^{-3}	3.74×10^{3}
97CM	−14.4	3.12×10^{-3}	4.62×10^{3}
80B IV	−9.85	1.78×10^{-3}	5.54×10^{3}
96AB	−7.75	1.55×10^{-3}	5.03×10^{3}
80B I	−7.00	1.16×10^{-3}	6.05×10^{3}
80B III	−4.88	6.24×10^{-4}	7.83×10^{3}
80B V	−3.82	4.81×10^{-4}	7.95×10^{3}
84A II	−3.32	4.01×10^{-4}	8.30×10^{3}
84A I	−3.14	4.05×10^{-4}	7.78×10^{3}
79ET	−3.10	4.36×10^{-4}	7.11×10^{3}

[a]Sample cut with $\vec{I} \parallel [11\bar{2}]$.

B. Model

Next we consider a model which presumably will indicate the pressure region in which thermal coupling between the Γ and L bands becomes small enough to allow an unambigious determination of the L-band Te-donor activation energy E_D. The model used is similar to those employed by Kosicki and Paul[5] and others[7,8] to explain pressure results on n-GaSb(Te). A first assumption is that Te-donor levels below the central minimum are merged with the band. The same donors produce N_D levels associated with the subsidiary L minima and have a nonzero ionization energy E_D. A concentration of $N_A = 10^{17}$ cm^{-3} singly ionizable acceptors is presumed to be present. If n_Γ, n_L, and n_i are the concentrations of carriers in the Γ minimum, L

minima, and the impurity levels associated with the L minima, respectively, the total carrier concentration N is given by

$$N = N_D - N_A = n_\Gamma + n_L + n_i$$
$$= N_{c\Gamma} F_{1/2}(\eta) + N_{cL} F_{1/2}(\eta - \Delta E/kT)$$
$$+ N_D/\{1 + \beta \exp[(\Delta E - E_D - E_F)/kT]\}, \quad (2)$$

where

$$\Delta E = \Delta E_0 + \frac{\partial \Delta E}{\partial P} P , \quad (3)$$

$$N_{c\Gamma} = 2(2\pi m_\Gamma^* kT/h^2)^{3/2} ,$$
$$N_{cL} = 2(2\pi m_{Ld}^* kT/h^2)^{3/2} , \quad (4)$$

and

$$m_{Ld}^* = \nu_L^{2/3} (m_\perp^{*2} m_\parallel^*)^{1/3} . \quad (5)$$

In Eq. (2), β is the degeneracy factor, $\eta = E_F/kT$ is the reduced Fermi energy, and E_F is related to the L-band edge. In Eq. (3), ΔE_0 is the separation between the Γ and L-band edges at $T = 0$ °K and atmospheric pressure ($P = 0$), and $\partial \Delta E/\partial P$ is assumed to be constant. A three-conduction-band model is assumed, and the electrical conductivity σ is given by

$$\sigma = \rho^{-1} = e(n_\Gamma \mu_\Gamma + n_L \mu_L + n_i \mu_i) , \quad (6)$$

where μ_Γ and μ_L are the electron mobilities in the Γ band and L band, respectivity; μ_i is the mobility ascribed to impurity conduction. The same model gives for the weak-field Hall coefficient[18]

$$R_H = -\frac{1}{e} \frac{n_\Gamma \mu_\Gamma^2 + F(K) n_L \mu_L^2 + n_i \mu_i^2}{(n_\Gamma \mu_\Gamma + n_L \mu_L + n_i \mu_i)^2} , \quad (7)$$

where $F(K) = 3K(K+2)/(2K+1)^2$ is the shape factor for [111] valleys, K is the anisotropy factor $(m_\parallel^* \tau_\perp)/(m_\perp^* \tau_\parallel)$ appropriate for these valleys, and the Hall factors r have been set equal to unity for each band. A list of the parameters used in the calculations is given in Table II.

Since the predictions of the model are to be compared to the behavior of sample 97CT, we choose $N = N_D - N_A = 9.6 \times 10^{16}$ cm^{-3}, consistent with the value of R_H ($T = 4.2$ °K, $P = 0$) given in Table I for this sample. Figures 4 and 5 give the results of computer calculations for various fixed pressures. As seen in Fig. 5, maxima in the Hall coefficient appear both at low and high pressures, with be-

TABLE II. Parameters of the model.

$m_\Gamma^* = 0.052 m_0$	$\mu_\Gamma = 2500$ cm^2/V sec
$m_{Ld}^* = 0.56 m_0$	$\mu_L = 500$ cm^2/V sec
$E_D = 20$ meV	$\mu_i = 10$ cm^2/V sec
$\Delta E_0 = 90$ meV	$\beta = 0.5$
$\partial \Delta E/\partial P = -10$ meV/kbar	$F(K) = 0.85$

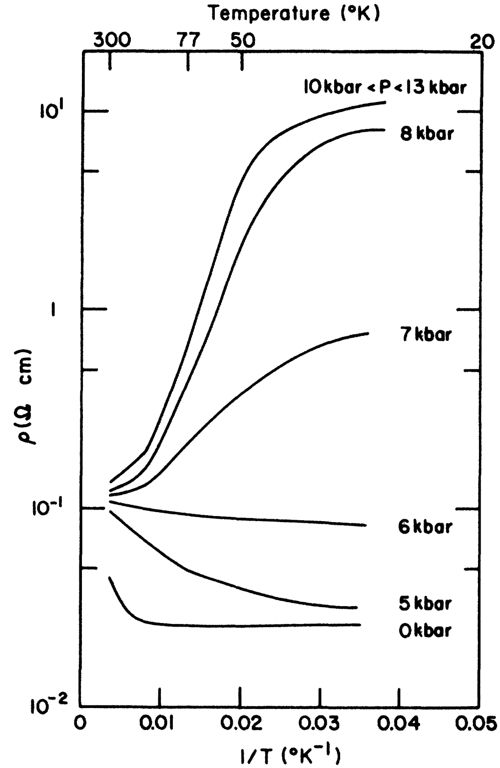

FIG. 4. Resistivity ρ vs reciprocal temperature calculated for the parameters listed in Table II.

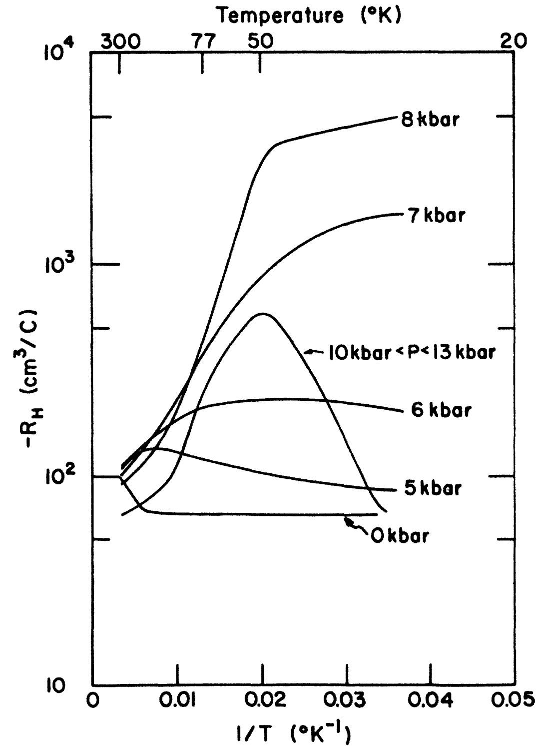

FIG. 5. Hall coefficient R_H vs reciprocal temperature calculated for the parameters listed in Table II.

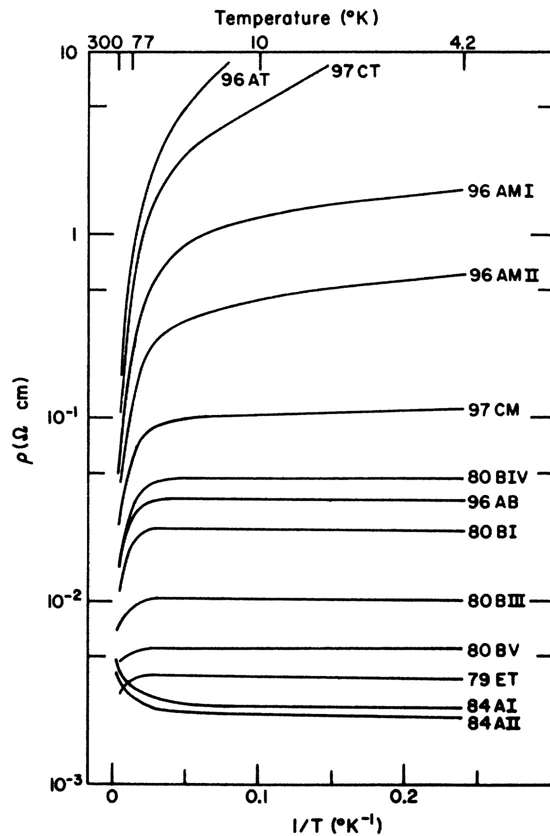

FIG. 6. Resistivity ρ vs reciprocal temperature for all samples listed in Table I.

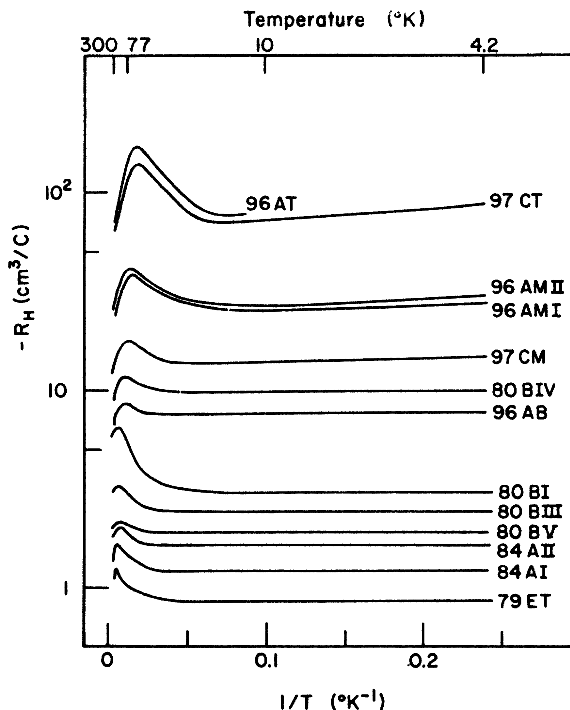

FIG. 7. Hall coefficient R_H vs reciprocal temperature for all samples listed in Table I.

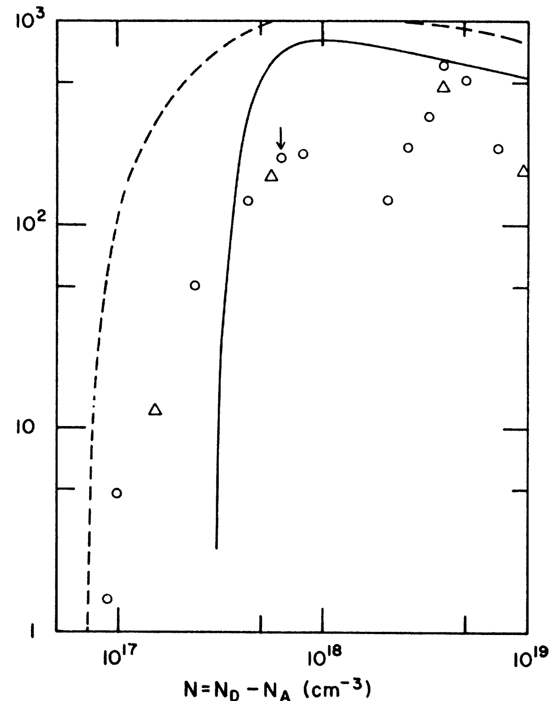

FIG. 8. Hall mobility μ_H vs $N = N_D - N_A$ at 4.2 °K. △, results of Ahlgren, Becker, and Stankiewicz (Ref. 9); ○, present results; dashed line, Sb-doped germanium results of Ceuvas and Fritzsche at 1.2 °K (Ref. 43); solid line, As-doped germanium results of Cuevas and Fritzsche at 1.2 °K (Ref. 44). The arrow indicates the position of the observed nonmetal-metal transition, as discussed in Sec. IV B.

havior at intermediate pressures qualitatively similar to the experimental results. In both figures, saturation in the behaviors of R_H and ρ occur for all pressures above ~10 kbar, consistent with the data.

According to an analysis by Blakemore[19] involving a simple model of an impurity semiconductor, the carrier concentration in the L band would be given by the expression

$$n_L \approx \beta N_{cL}[(N_D - N_A)/N_A] \exp(-E_D/kT) \tag{8}$$

for the case $n_L \ll N_A \ll N_D$. The computer calculations for our model indicate that this condition holds for the temperature range $50 < T < 77$ °K. Thus, for the case of $\mu_L \gg \mu_i$, and μ_L independent of temperature,

$$\rho \sim \rho_0 e^{E_D/kT} \tag{9}$$

in this temperature range for $P > 10$ kbar. For sample 97CT, the activation energy for resistivity data over the range $50 < T < 77$ °K and $P > 10$ kbar is 13.2 meV. The effects of pressure changes in the sealed bomb at higher temperatures have not been introduced into the calculations. Inspection of the curves given in Figs. 4 and 5 suggest that

some of the features of the high-temperature data for $P < P_s$ may be related to such effects. For example, in Fig. 1, the small relative maximum in ρ vs T^{-1} for P (300 °K) ≅ 9.5 kbar may be inferred from the fixed-pressure curves of Fig. 4 by including a ~3-kbar decrease in pressure over the range $300 > T > 150$ °K. The model thus appears to be qualitatively correct, furthermore, it is useful in predicting the pressure range of thermal decoupling of the Γ and L bands.

C. Survey of sample behaviors for $P > P_s$

1. $\rho(T)$ and $R_H(T)$

The behavior of ρ and R_H for all samples listed in Table I are shown in Figs. 6 and 7. In every case, the curves plotted correspond to $P > P_s$ at all temperatures; experimentally P_s (300 °K) ~ 11 kbar and P_s (4.2 °K) ~ 8 kbar. The experimental behavior in the resistivity seen at low temperatures in low-concentration samples is presumed to be related to impurity conduction, whereas the high-temperature behavior is dependent on ionization from the Te-donor levels into the associated L-band states. As seen in Fig. 6, the impurity activation energy apparently decreases with increasing concentration. For two samples, 84AI and 84AII, the resistivity *decreases* with decreasing temperature. In a still higher-concentration sample, 79ET, a small activation energy reappears. This apparently anomalous behavior may be explained by considering the mobility ratio μ_L/μ_i. In lower-concentration samples and in sample 79ET, $\mu_L/\mu_i > 1$, and deionization should be accompanied by an *increase* in resistivity. For samples 84AI and 84AII, the ratio $\mu_L/\mu_i < 1$, and deionization leads to a *decrease* in resistivity. The appearance of Hall maxima in all samples is not inconsistent with this interpretation, since the ratio given by Eq. (1) does not establish which of the two carrier mobilities is largest. An increase in the Hall-coefficient maximum and shift to higher temperatures is seen in sample 80BI, as compared to samples of similar concentration. This result is ascribed to an anomalously low value of μ_i, and a greater value of the ratio μ_L/μ_i than in samples of only slightly different concentration.

2. μ_H (4.2°K)

In Fig. 8, we plot the 4.2 °K Hall mobility μ_H vs $N = N_D - N_A$. In low-concentration samples, N is taken directly from R_H (4.2 °K, $P=0$), whereas the value of N is taken from R_H (4.2 °K, $P > P_s$) for high-concentration samples assuming all carriers are in an impurity band. The behavior observed is similar to results obtained in Sb- and As- doped germanium; these are also plotted in Fig. 8. As seen in the figure, the mobility dependence on the uncompensated donor concentration $N_D - N_A$ is intermediate between that of Sb and As doping. Considerable scatter is noted in mobility values for high-concentration n-GaSb(Te) samples. It was determined that the scatter was not due to macroscopic inhomogeneities; this behavior was not studied further because of limited sample availability.

3. Ratio of Hall coefficient at $P > P_s$ and $P = 0$

Ahlgren, Becker, and Stankiewicz[9] and Ahlgren[18] noted that the ratio $\gamma = [R_H\ (P > P_s)/R_H\ (P=0)]_{4.2\,°\mathrm{K}}$ is approximately unity in an intermediate concentration sample R_H (4.2 °K, $P=0$) = − 11 cm³/C, but falls well below unity (0.23, 0.46) in the highest-concentration samples investigated [R_H(4.2 °K, $P=0$) = − 2.82, − 3.52 cm³/C]. (In our lowest-concentration samples, γ cannot be determined because of lack of interpretation of the Hall coefficient for impurity conduction.) Figure 9 gives γ as a function of R_H (4.2 °K, $P=0$) for samples used in the present investigation, as well as the samples discussed by Ahlgren *et al.* As seen in the figure, γ drops precipitously at $7 \leq |R_H| \leq 7.75$. A further decrease is noted for $|R_H| \lesssim 3$cm³/C. The Fermi-energy shift over this range of R_H is ~25 meV using a constant mass of $m^* = 0.052 m_0$. For a nonparabolic band, the shift is ~16.5 meV, assuming the parameters given by Yep and Becker.[20] The results suggest that resonance states lie approximately 20 meV below the L-band edge; these states are then presumed to be the states associated with the high-temperature activation energy seen in the resistivity plots in Fig. 6. At the

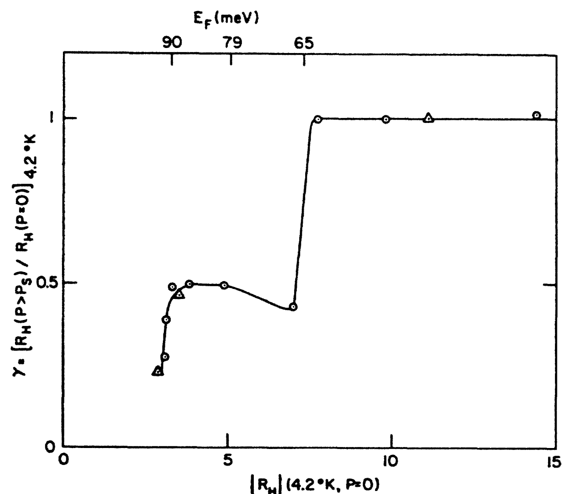

FIG. 9. Ratio of Hall coefficients $\gamma = [R_H(P > P_s)/R_H (P=0)]_{4.2\,°\mathrm{K}}$ vs $|R_H|$ (4.2 °K, $P=0$) for intermediate- and high-concentration samples. △, results of Ahlgren, Becker, and Stankiewicz (Ref. 9); ○, present results. E_F is given relative to the Γ-band edge at $P=0$; the values are estimated using $m^* = 0.052 m_0$.

highest concentrations, the further decrease in γ may be evidence for the filling of L-conduction-band states.

4. $\mu_H(T)$

Figure 10 gives the temperature dependence of the Hall mobility for representative samples. At 4.2 °K extremely low mobilities characteristic of impurity conduction are seen in the low-concentration sample 96AT. As the concentration rises, the mobility approaches temperature-independent behavior at low temperatures. Further increases occur at higher concentration and the mobility of impurity conduction reaches values at low temperature which are comparable to the room-temperature mobility presumably characteristic of L-band conduction. The maxima in the mobilities exhibited near room temperature suggest that lattice scattering of L-band carriers dominates at still higher temperatures. The experimental values of μ_H at 300 °K are close to previous estimates of the L-band mobility. In general, the 300 °K mobility at $P > P_s$ decreases with increasing concentration.

5. Magnetoresistance behavior

Magnetoresistance data for cubic crystals is interpretable in terms of the phenomenological theory of Seitz.[21] To second order in B, the final result is stated in the form

$$M_{ijk}^{lmn} \equiv (\Delta\rho/\rho_0 B^2)_{ijk}^{lmn} = b + c\left(\sum \iota\,\eta\right)^2 + d\sum \iota^2\eta^2 , \quad (10)$$

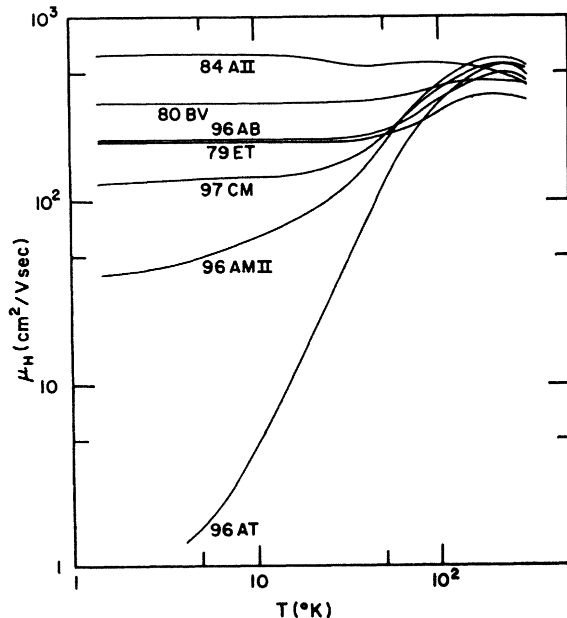

FIG. 10. Hall mobility μ_H vs temperature for various representative samples. The data points are deleted for the sake of clarity.

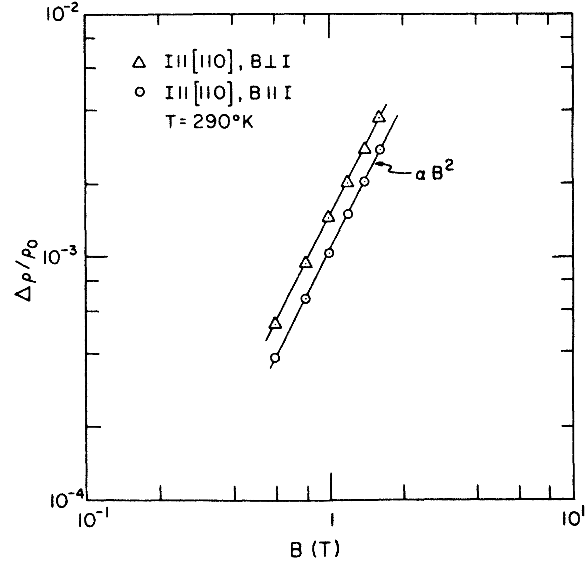

FIG. 11. Transverse and longitudinal magnetoresistance vs magnetic field strength at T = 290 °K for sample 96AM II.

where $\Delta\rho$ is the change in resistivity from the zero-field value ρ_0, due to the magnetic field B, and ι and η are the direction cosines of the current and magnetic field vectors with respect to the cubic axes. The coefficients b, c, and d are constants of the material which depend on the band structure and carrier relaxation processes. The theory is applicable only under weak-field conditions $\mu B \ll 10^4$, where the mobility μ is in cm²/V sec and B is in teslas.

The magnetoresistance behavior of several samples was examined in detail at various temperatures for $P > P_s$. Measurements were mainly confined to the temperature range over which L-band conduction appears to dominate.

The three samples investigated 96AMI, 96AMII, and 97CM all showed B^2 dependence of the resistance both in the longitudinal and transverse configurations, over the complete range from 77 to 295 °K and in fields up to 1.6 T. Typical behavior is seen in Fig. 11. For sample 96AMII, two current–magnetic-field orientations were studied: (i) $\vec{I} \parallel [110]$, $\vec{B} \perp \vec{I}$, and (ii) $\vec{I} \parallel [110]$, $\vec{B} \perp [1\bar{1}0]$. For case (i), Eq. (10) may be rewritten in the form

$$\Delta\rho/\rho_0 B^2 = (b + \tfrac{1}{4}d) - \tfrac{1}{4}d\cos 2\theta , \quad (11)$$

where θ is the angle between $\vec{B}$ and the [001] direction. The experimental result for this orientation is shown in Fig. 12; the smooth curve represents a least-squares fit to the data using the parameters listed in Table III. For case (ii), Eq. (10) may be rewritten in the form

$$\Delta\rho/\rho_0 B^2 = (b + \tfrac{1}{2}c + \tfrac{1}{4}d) + (\tfrac{1}{2}c + \tfrac{1}{4}d)\cos 2\phi , \quad (12)$$

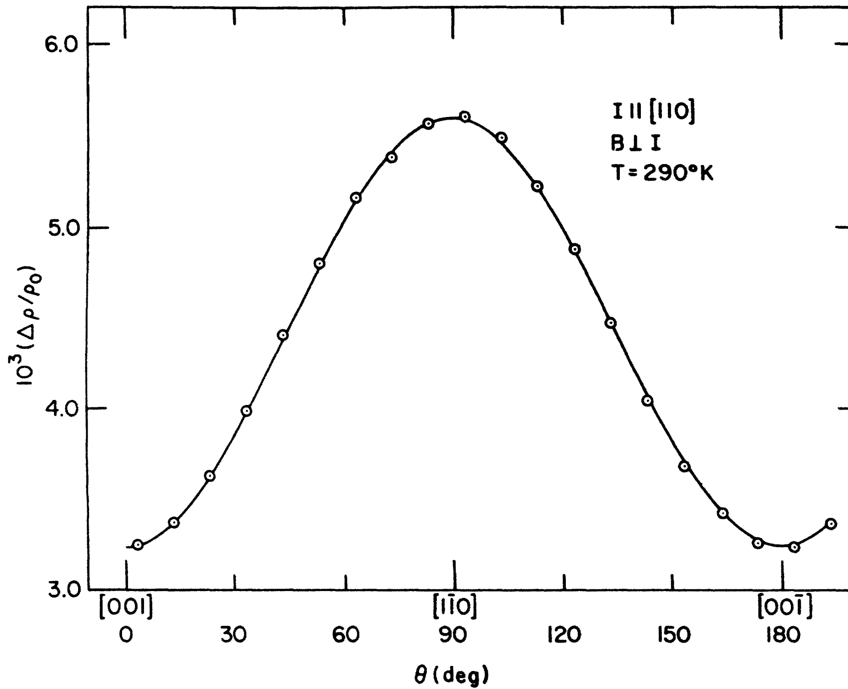

FIG. 12. Angular variation of transverse magnetoresistance at $T = 290$ °K and $B = 1.5$ T for sample 96AM II.

where ϕ is the angle between $\vec{B}$ and $\vec{I}$. The experimental result for this orientation is shown in Fig. 13, with the fit performed as in Fig. 12. Cryogenic baths were used for the measurements at 77 and 195 °K, whereas the data at 95, 116, and 161 °K were obtained during slow warmings of the bomb. Ideally, the relations between the Seitz coefficients b, c, and d are obtained from a single sample without remounting the sample; the current-field orientations in sample 96AMI allowed such measurements. As seen in Table III, the room-temperature results for 96AMII, where two sample mountings were required to derive the three Seitz coefficients, are in close agreement with the results listed for sample 96AMI. In both cases, the relations indicative of [111] valleys hold, namely, $b + c = 0$ and $d > 0$.

IV. ANALYSIS AND DISCUSSION

A. Activation energies

A number of investigators have obtained the Te-donor activation energies in GaSb from an analysis of hydrostatic-pressure measurements at fixed

TABLE III. Seitz coefficients, anisotropy parameters, and scattering factors of various samples for $P > P_s$.

Sample	$\vec{I}$	$\vec{B}$	T (°K)	μ_H (cm^2/V sec)	b (10^{-3} T^{-2})	d (10^{-3} T^{-2})	c (10^{-3} T^{-2})	q	K_+	A
96AM I	$\parallel[\bar{1}\bar{1}2]$	$\perp[\bar{1}10]$	295	480	1.49	1.95	−1.34	3.91[a]	6.56	1.4
								3.74[b]	6.99	1.32
			77	165	0.97	−0.78	0.22	···	···	···
96AM II	$\parallel[110]$	$\perp[110]$ $\perp[\bar{1}10]$	290	547	1.44	2.09	−1.39	4.18	5.96	1.24
		$\perp[110]$	195	598	2.00	2.67	···	4.17	5.98	1.33
		$\parallel[\bar{1}10]$	161	580	2.00	2.51	···	4.27	5.79	1.36
		$\parallel[001]$	116	492	1.87	1.60	···	5.36	4.45	1.56
			95	428	1.76	0.76	···	9.42	2.86	1.81
		$\perp[110]$ $\perp[\bar{1}10]$	77	360	1.53	~0.078	~1.16	···	···	···
97CM	$\parallel[110]$	$\perp[110]$	295	480	1.74	1.83	···	4.42	5.54	1.50
			77	322	3.93	1.18	···	8.44	3.07	4.38
									8.6[c]	

[a]Calculated from b and d. [b]Calculated from c and d. [c]Reference 23.

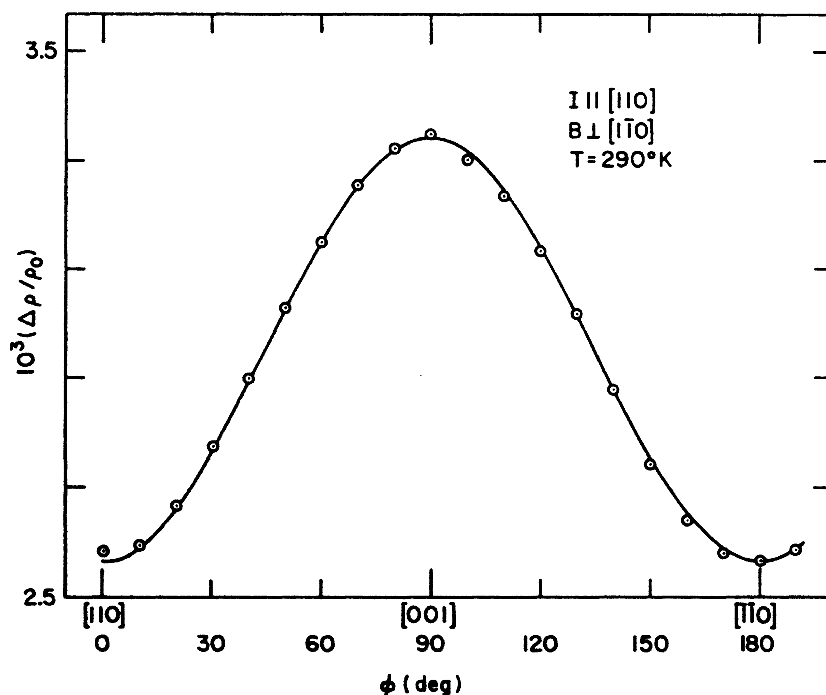

FIG. 13. Angular variation of magnetoresistance at $T = 290\,°K$ and $B = 1.5$ T for sample 96AM II.

temperature. Kosicki[5] derived a value of $E_D = 0.02$ eV from 77 °K resistivity data on a low-concentration sample ($n \sim 1.7 \times 10^{17}$ cm^{-3}) using pressures up to 10 kbar. Additionally, Kosicki interpreted photoluminescence results in terms of a pressure-induced separation of the Te-donor level initially degenerate with the Γ band at $P = 0$; the analysis gave an increase of the activition energy to 0.02 eV at 10 kbar. Pitt[7] found that resistance versus pressure data at 300 °K for a sample of intermediate concentration ($n \sim 4.75 \times 10^{17}$ cm^{-3}) can be explained using a constant L-band donor energy of $E_D = 0.020 \pm 0.005$ eV. Kosicki[5] saw evidence in n-GaSb(Se) that the L-band Se-donor activation energy might be a function of pressure below a critical pressure P_c. However, he did not invoke this same mechanism in the case of the equivalent resonant state in n-GaSb(Te), presumably because of the insensitivity of the experimental results to this refinement in the model. Our present results do not indicate that pressure affects the degeneracy of the Γ-band Te-donor level. Also, our model can be used to show that if the L-band Te-donor level shifts with pressure for $P < P_s$, the effect is obscured by the thermal coupling of the bands. The results to be discussed below therefore relate only to the L-band activation energies of bound states for $P > P_s$.

Assuming a hydrogenic nature for the donor impurities, we estimate the thermal ionization energy from the expression[22]

$$E_D = (m^*/m_0)(13.6/\epsilon_0^2), \qquad (13)$$

where the static dielectric constant $\epsilon_0 = 15.7$, and $m^* = (m_\parallel^* m_\perp^{*2})^{1/3}$. For a value of $m^* = 0.287 m_0$ (estimated from $K_m = 8.6$ and $m_\perp^* = 0.14 m_0$),[23] we find $E_D = 15.7$ meV, in fair agreement with the results obtained on sample 96AT, namely, $\epsilon_1 = 13.8$ meV. The hydrogenic model assumes an isotropic effective mass. In the effective-mass approximation, the anisotropic effective mass is employed in the Schrödinger equation. An estimate of E_D based on the effective-mass approximation[24] and employing the parameters used in the hydrogenic model gives $E_D = 14$ meV.

Early experimental work on Ge and Si suggested that the activation energy of shallow impurities decreases with increasing concentration. Pearson and Bardeen[25] fit their results to the empirical equation

$$E_D = E_D(0) - \alpha N_D^{1/3}, \qquad (14)$$

where α is a constant, and $E_D(0)$ is the ionization energy at infinite dilution. For p-type Si, they found $\alpha = 4.3 \times 10^{-8}$ eV cm. Later, Debye and Conwell[26] argued that N_D should be replace by N_{di}, where N_{di} is the average density of ionized majority impurities in the low concentration or low-temperature region. Their analysis on n-type Ge gave $\alpha = 2.35 \times 10^{-8}$ eV cm, also using Eq. (14).

In Fig. 14, we present the experimental results listed in Table IV. N_D is calculated from Hall data assuming $N_A \doteq 1 \times 10^{17}$ cm^{-3}. A least-squares fit to Eq. (14) gives ϵ_1 ($N_D \to 0$) $= E_D(0) = 18.0$ meV and $\alpha = 9.7 \times 10^{-9}$ eV cm to within 5%. Using the approach

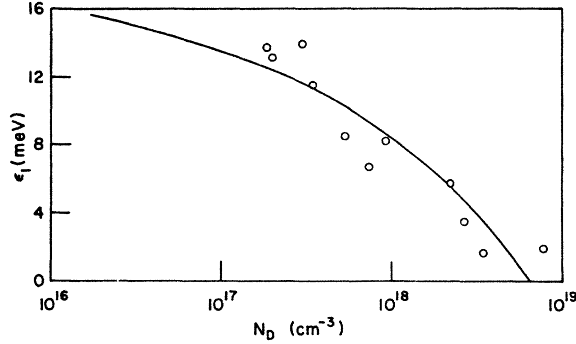

FIG. 14. Activation energies of Te donor states associated with the L band. Solid Line, plot of ϵ_1 vs $N = N_D - N_A$ according to Eq. (14).

of Debye and Conwell, N_{di} for each sample is calculated from the model described in Sec. III B, with the experimental value of ϵ_1 being employed as a first approximation to E_D. Fitting Eq. (14) only to the experimental results for the lowest- and highest-concentration samples, we obtain $E_D(0) = 17.4$ meV and $\alpha = 8.0\times10^{-9}$ eV cm. These results should only be considered as suggestive, since the low-concentration range $[(N_D - N_A) < 10^{17}\ \text{cm}^{-3}]$, i.e., the region in which the theory is presumed valid, is not accessible in n-GaSb(Te) with present growth techniques. Furthermore, at high concentrations, several mechanisms may give ϵ_1 values considerably below E_D. These are (i) departures from the conditions outlined for the validity of Eq. (8), and (ii) conductivity contributions from impurity conduction. For mechanism (i), at very high donor concentrations the carrier density may satisfy the relation $N_A \ll n_L \ll N_D$ in the region where impurity ionization into the L band is taking place. In this case, Blackmore[19] shows that

$$n_L \approx (\beta N_{cL} N_D)^{1/2} \exp(-E_D/2kT). \tag{15}$$

Thus the apparent activation energy seen in the resistivity would be reduced to one-half the true activation energy. [Incorporation of this feature in evaluating the data leads to the 5% uncertainty in $E_D(0)$ and α quoted earlier.] Direct evidence for the presence of (ii) is the resistivity behavior in samples 84AI and 84AII, where the influence of impurity conduction apparently extends to unexpectedly high temperatures. Indeed, the reappearance of an activated region in the resistivity, seen in 79ET, is a fortuitous consequence of a drop in the mobility of impurity conduction.

B. Mobility

We consider four scattering mechanisms in calculating the mobility of the L-band carriers. There are, polar-optical, acoustic-mode, ionized-impurity, and neutral-impurity scattering. We take the approach that the total mobility μ_{tot} is given approximately by

$$\frac{1}{\mu_{\text{tot}}} = \frac{1}{\mu_{po}} + \frac{1}{\mu_{am}} + \frac{1}{\mu_I} + \frac{1}{\mu_N}. \tag{16}$$

Equation (16), which is based on Matthiessen's rule, is known to be inaccurate when, for example, the lattice and impurity-scattering rates are comparable in magnitude.[27] From the following analysis, we find that at the end points of the temperature range considered (between 77 and 300 °K), only one scattering mechanism is dominant, and Eq. (16) is a reasonable approximation at these points. A more rigorous calculation over the complete temperature range, involving averages of the relaxation times over the distribution function, appears to be premature because of lack of knowledge of material properties.

1. Polar-optical scattering

The mobility for polar-optical scattering is given by[28]

$$\mu_{po} = 0.199(T/300)^{1/2}(e/e_c^*)^2(m_0/m^*)^{3/2} \times (10^{22}M_r)(10^{23}V_a)(10^{-13}\omega_l)(e^z - 1) \times [e^{-\eta}G_1(z)]\ \text{cm}^2/\text{V sec}, \tag{17}$$

where e_c^* is the effective ionic charge as defined by Callen,[29] M_r is the reduced mass of the two ions in the unit cell, V_a is the volume of the unit cell, ω_l is the longitudinal optical frequency, η is the reduced Fermi energy E_F/kT, and $z = \hbar\omega_l/kT$. The quantity $e^{-\eta}G_1(z)$ is a slowly varying function of z of the order unity which is given in graphical form by Howarth and Sondheimer.[30] For a many-valley semiconductor, agreement to within 10% of the exact treatment is obtained when the mass dependence $(m^*)^{-n}$ is replaced by[31]

TABLE IV. Uncompensated donor concentrations and activation energies of various samples.

Sample	$N = N_D - N_A$ (cm^{-3})	ϵ_1 (meV)
96AT	8.87×10^{16}	13.8
97CT	9.62×10^{16}	13.2
96AM I	2.06×10^{17}	14.0
96AM II	2.44×10^{17}	11.5
97CM	4.34×10^{17}	8.5
80BIV	6.35×10^{17}	6.8
96AB	8.07×10^{17}	8.2
80B I	2.08×10^{18}	5.8
80B III	2.57×10^{18}	3.5
80B V	3.29×10^{18}	1.7
84A II	3.86×10^{18}	···
84A I	5.12×10^{18}	···
79ET	7.27×10^{18}	1.9

$$(m^*)^{-n} \rightarrow \tfrac{1}{3}[(m_\parallel^*)^{-1}+2(m_\perp^*)^{-1}][(m_\parallel^*)(m_\perp^*)^2]^{-(n-1)/3}. \quad (18)$$

2. Acoustic-mode scattering

Bardeen and Shockley[32] have given a formula for the mobility due to acoustic-mode scattering. Their result is

$$\mu_{am}=\frac{(8\pi)^{1/2}}{3}\,\frac{e\hbar^4\rho v_l^2}{(kT)^{3/2}(m^*)^{5/2}E_1^2}$$

$$=3.0\times10^{-5}\rho v_l^2(m_0/m^*)^{5/2}/T^{3/2}E_1^2 \text{ cm}^2/\text{V sec}, \quad (19)$$

where ρ is the density, v_l is the sound velocity of the longitudinal wave, and E_1 is the deformation potential. The mass m^* is calculated as in Eq. (18).

3. Ionized-impurity scattering

According to the Brooks-Herring theory,[33] the mobility due to ionized-impurity scattering is

$$\mu_I=\frac{2^{7/2}(kT)^{3/2}\epsilon_0^2}{\pi^{3/2}e^3(m^*)^{1/2}N_I}\left[\ln\left(\frac{6m^*(kT)^2\epsilon_0}{\pi e^2\hbar^2 n'}\right)-1\right]^{-1}, \quad (20)$$

where

$$n'=n+[1-(n+N_A)/N_D](n+N_A).$$

N_I is the total number of ionized impurities and is weighted by the appropriate charge state, i.e., $N_I=\sum_i N_i Z_i^2$. For singly charged acceptors and donors, $N_i=n+2N_A$. In Sec. III B, only singly ionized acceptors were considered in the model. The work of Baxter, Reid, and Beer[34] suggests that the residual acceptors in GaSb may be doubly ionizable. In this case, the weighting leads to $N_I=n+6N_A$. We assume this latter weighting in our estimates for ionized-impurities scattering.

The value of μ_I is relatively insensitive to the choice of effective mass appearing in the logarithmic term in Eq. (20), and the conductivity effective mass has been employed for this term. The effective mass appearing as $(m^*)^{-1/2}$ in the prefactor in Eq. (20) is evaluated according to a suggestion by Smith.[35] Whether this procedure is correct is not known for L-band carriers in GaSb. A more correct procedure has been employed by Norton, Braggins, and Levinstein[36] in an investigation on n-Si. In their study, the relaxation-time anisotropies are decomposed into their separate contributions along and perpendicular to the valley axis and the appropriate mass component to be used is given unambiguously. Such calculations do not appear to be appropriate for GaSb as yet, since the preliminary question of the charge state of the acceptor which is of overwhelming importance in determining μ_I in n-type material is not settled. For example, if the acceptors are only single charged, the value of μ_I is more than doubled as compared to the doubly ionized state. Norton, Braggins, and Levinstein[36] in discussing the failure of Brooks-Herring formula, state that the theory overestimates the strength of ionized-impurity scattering, thus suggesting that a correct calculation would give a larger mobility than calculated from Eq. (20). Clearly, a stronger rather than a weaker scattering mechanism is required to explain the 77 °K mobility value for sample 97CT.

4. Neutral impurity scattering

Neutral impurity scattering should be important at low temperatures for $P>P_s$, as contrasted with the $P=0$ case, since impurity deionization is a prominent feature of the high-pressure data. The mobility for this scattering mechanism has been given by Erginsoy as follows,[37]

$$\mu_N=\frac{e^3m^*}{20\hbar^3\epsilon_0N_N}=1.435\times10^{22}\times(m^*/m_0)/\epsilon_0N_N \text{ cm}^2/\text{V sec}, \quad (21)$$

where N_N is the number of neutral donors (referring to Sec. III B, $n_i=N_N$).

The parameters used in the estimates of the individual mobility contributions are listed in Table V; the results are given in Table VI for sample 97CT and 300 and 77 °K. By comparing the calculated values with the experimental results for this sample, it is seen that acoustic-mode scattering is dominant at 300 °K, whereas at 77 °K scattering is mainly due to ionized impurities. For sample 96AB, the impurity-scattering contribution at 300 °K increases as compared to 97CT, but is still small relative to acoustic-mode scattering.

For $P>P_s$, a two-band model for conduction in both the L band and an impurity band gives[38]

$$\mu_{\text{tot}}=\frac{n_L\mu_L^2+n_i\mu_i^2}{n_L\mu_L+n_i\mu_i}. \quad (22)$$

If $n_L\gg n_i$, μ_{tot} represents the mobility of L-band carriers, whereas if $n_i\gg(\mu_L/\mu_i)^2n_L$, the measured mobility should be that of impurity conduction. Previous workers have discussed an intermediate situation where

$$n_L(\mu_L/\mu_i)^2>n_i>n_L(\mu_L/\mu_i), \quad (23)$$

in which case

$$\mu_{\text{tot}}=(n_L/n_i)(\mu_L^2/\mu_i). \quad (24)$$

In low-concentration samples, ionized impurity scattering dominates at low temperatures leading to $T^{3/2}$ dependence for μ_L. Equation (24) suggests that the measured Hall mobility decreases more rapidly than $T^{3/2}$ due to the decreasing ratio of n_L/n_i as the temperature is lowered. Some evidence of this behavior is seen for both 97CT and 96AT, but the effect is rather weak compared to its importance in other materials.[38]

According to a recent calculation by Martino, Lindell, and Berggren[39] on nonmetal-metal transitions in n-type many-valley semiconductors, n_c, the critical density for the transition occurs at $n_c^{1/3} a_H \simeq 0.305$ for a four-valley system, where the first Bohr radius $a_H = \hbar^2 \epsilon_0 / m^* e^2$. This result is obtained by numerical integration of the radial Schrödinger equation using a Hubbard-Sham dielectric screening function. Krieger and Nightingale[40] used a 1s hydrogenic orbital, a variational calculation, and a Lindhard dielectric screening function to predict the transition. For both calculations, the many valley aspect of the calculation is introduced through the screening function. The Krieger-Nightingale theory[40] gives $n_c^{1/3} a_H = 0.23$, in good agreement with Mott's theory for an isotropic single valley,[41] namely, $n_c^{1/3} a_H \simeq 0.25$. Since we obtain good agreement with the experimentally observed ionization energy in the purest sample using the hydrogenic model, we assume also that the first Bohr orbit radius can be calculated using the geometric mass $m^* = (m_\parallel m_\perp^2)^{1/3}$ of a single L valley. Insertion of the L-band parameters presented in Table V yields $n_c = 1.16 \times 10^{18}$ cm^{-3} for the result given by Martino *et al.*,[39] and $n_c = 5 \times 10^{17}$ cm^{-3} for the Krieger-Nightingale prediction.[40] According to the criterion stated by Fritzsche,[42] nonmetal-metal transitions occur in semiconductors when the activation energy ϵ_2 in the resistivity vanishes. For n-GaSb(Te), this apparently takes place at a concentration of $\sim 6 \times 10^{17}$ cm^{-3} for $P > P_s$. As in donor-doped Ge,[43,44] our results appear to be in agreement with the Krieger-Nightingale theory rather than with the theory of Martino *et al.*

TABLE V. Values of parameters used for L-band mobility calculations.

Parameter	Values
e_c^*	$0.13e$ [a]
V_a	2.268×10^{-22} cm^3 [b]
M_r	7.36×10^{-23} g [b]
ω_l	3.324×10^{13} sec^{-1} [c]
$m_\parallel^*$	$1.2 m_0$ [d]
$m_\perp^*$	$0.14 m_0$ [d]
ϵ_0	15.7 [e]
ρ	5.614 g/cm^3 [f]
v_l	4.298×10^5 cm/sec [f]
E_1	13.6 eV [g]

[a] C. Hilsum, in *Semiconductors and Semimetals*, edited by R. K. Willardson and A. C. Beer (Academic, New York, 1966), Vol. 1, p. 16.
[b] C. Hilsum and A. C. Rose-Innes, *Semiconducting III-V Compounds* (Pergamon, New York, 1961).
[c] S. S. Mitra, Phys. Rev. 132, 986 (1963).
[d] Reference 23.
[e] *American Institute of Physics Handbook*, 3rd ed. (McGraw-Hill, New York, 1972), p. 9–73.
[f] H. J. McSkimin, A. Jayaraman, P. Andreach, and T. B. Bateman, J. Appl. Phys. 39, 4127 (1968).
[g] Reference 22, p. 146.

TABLE VI. Calculated L-band mobility values for different scattering mechanisms and experimental result for sample 97CT at $P > P_s$.

	300 °K (cm^2/V sec)	77 °K
μ_{po}	5.55×10^3	6.97×10^4
μ_I	2.35×10^3	5.20×10^2
μ_{am}	1.06×10^3	8.15×10^3
μ_N	8.63×10^4	4.70×10^3
μ_{tot}	640	440
μ_H(expt)	520	270

In analogy with the data for Sb- and As-doped n-type Ge,[43,44] a fall-off in mobility at high Te concentrations is expected at low temperatures in n-GaSb(Te). This behavior is usually analyzed in terms of the mobility dependence on concentration N and Fermi energy E_F, e.g.,

$$\mu \propto N^r E_F^s ,$$

where r and s are parameters to be determined from the data. The scatter in the mobility results seen in Fig. 8 rules out the determination of these parameters. However, the general trend of the results is consistent with the Ge data of Cuvas and Fritzsche.[43,44]

In a series of papers on the analysis of the low-temperature resistivity of unstrained and uniaxially stressed n-type degenerately doped Ge, Krieger *et al.*[45–47] compared the predictions of the Brooks-Herring scattering theory to experimental results. It was found that in unstrained As-doped Ge,[48] the resistivity versus concentration data may be satisfactorily explained by correcting the Brooks-Herring theory through the use of anisotropic scattering and dielectric screening. Since we have previously noted that the Fermi level is probably below the L-band edge even in the highest-concentration samples of n-GaSb(Te) available to us, and since the scatter in the data is considerable, we have not considered a further analysis of the mobility results based either on the Cuevas and Fritzsche type of analysis[42,43] or on the considerations of Krieger *et al.*[45–47]

A preliminary examination of Fig. 8 suggests that at low concentrations the rise in mobility of n-GaSb(Te) with increasing N is more gradual than in Ge. Our instrumental limitations prevented Hall-effect measurements below ~ 4 °K, so that a direct comparison between n-GaSb(Te) and Ge is not available at 1.2 °K. However, the trends in the resistivity data for $T < 4$ °K suggest that the sharp increase in μ_H with N seen in Sb- and As-doped Ge probably also occurs in n-GaSb(Te) at

1.2 °K.

With $N_A \simeq 1\times10^{17}$ cm^{-3}, the estimated compensation ratio N_A/N_D in the lowest-concentration samples is $\simeq 0.5$. The irradiation studies of Davis and Compton[49] indicate that in Sb-doped Ge, ϵ_2, the activation energy in the so-called "intermediate concentration range" for impurity conduction, and ϵ_3, the activation energy for the so-called "low-concentration range," as well as the corresponding extrapolated resistivities $\rho_2(0)$ and $\rho_3(0)$, are strong functions of compensation. Since the compensation dependence of these features of the resistivity are not yet known in n-GaSb(Te), the comparison between the Ge and GaSb behaviors in these concentration regions should only be considered as preliminary in nature.

C. Magnetoresistance

Abeles and Meiboom[50] and Shibuya[51] solved the Boltzmann equation to second order in B for ellipsoidal energy surfaces and relaxation time dependent on energy only. Expressions for the magnetoconductivity coefficients were obtained which depend on the positions of the energy minima in k space. Herring and Vogt[52] extended the results for the case of anisotropic relaxation time τ when τ has the same symmetry as the energy ellipsoids. These can be put in the general form

$$M_{ijk}^{lmn} = A[F(K)]_{ijk}^{lmn} - 1 \tag{25}$$

and

$$M_{ijk} = A[F(K)]_{ijk} . \tag{26}$$

The absence of a subscript in Eq. (26) implies that the current and magnetic field are colinear.

Following Herring and Vogt,[52] we assume that the relaxation time anisotropy may be expressed in the form

$$\tau_{\parallel} = \tau_{\parallel}^0\,\tau(\epsilon), \quad \tau_{\perp} = \tau_{\perp}^0\,\tau(\epsilon) ,$$

where the energy dependence of $\tau(\epsilon)$ is the same for both components; the relaxation-time anisotropy $K_\tau = \tau_{\parallel}^0/\tau_{\perp}^0$ is then independent of energy, as is $K = K_m/K_\tau = (m_{\parallel}^*/m_{\perp}^*)(\tau_{\perp}^0/\tau_{\parallel}^0)$. The coefficient A which contains the transport integrals, is given by

$$A = \frac{\langle\tau(\epsilon)\rangle\langle\tau^3(\epsilon)\rangle}{\langle\tau^2(\epsilon)\rangle^2} , \tag{27}$$

where

$$\langle\tau^i(\epsilon)\rangle = \int_0^\infty \epsilon^{3/2}\,\tau^i(\epsilon)\frac{\partial f_0}{\partial\epsilon}\,d\epsilon \Big/ \int_0^\infty \epsilon^{3/2}\,\frac{\partial f_0}{\partial\epsilon}\,d\epsilon , \tag{28}$$

and f_0 is the zero-field Fermi distribution function.

Exact expressions for $F(K)$ for the special cases of ellipsoids centered along the [100], [111], and [110] directions in k space have been given in the literature.[53] All experimental results to date indicate [111] symmetry, leading to the choice of $F(K)$ mentioned in Sec. III B. Combining Eqs. (10), (25), and (26) for the case of [111] symmetry leads to the following expressions for the inverse Seitz coefficients:

$$b = -c = \mu^2\left(A\,\frac{(2K+1)^2}{3K(K+2)} - 1\right) \tag{29}$$

and

$$d = \mu^2 A\,\frac{(2K+1)(K-1)^2}{3K(K+2)^2} . \tag{30}$$

Combining (29) and (30), we obtain

$$q \equiv \left(1+\frac{b}{\mu^2}\right)\frac{2\mu^2}{d} = (K+2)(2K+1)/(K-1)^2 . \tag{31}$$

The two roots of the quadratic in K are

$$K_\pm = \frac{(5+2q)\pm(36q+9)^{1/2}}{2(q-2)} . \tag{32}$$

We initially assume that $\tau_{\parallel}/\tau_{\perp} = 1$. The choice K_+ leads to $K_m = (m_{\parallel}^*/m_{\perp}) > 1$ for the values of b, c, d, and μ found near room temperature, implying prolate ellipsoids. As seen in Table III, the values of K_+ and A show no definite trends from sample to sample at room temperature. As discussed earlier, the dominant scattering mechanism at 300 °K is acoustic-mode scattering. We assume from the consistency of the results at room temperature that additional scattering mechanisms related to impurity concentration are not important at this temperature.

At lower temperatures, our calculations indicate that impurity scattering dominates. For classical statistics and ionized-impurity scattering ($\tau\propto\epsilon^{3/2}$), $A = 1.58$. The corresponding values of A for acoustic-mode scattering ($\tau\propto\epsilon^{-1/2}$) and neutral impurity scattering are $A = 1.27$ and $A = 1.0$, respectively. It can be shown that for any admixture of energy-dependent scattering, mechanism $A \geq 1$. The A values listed in Table III for $T \geq 116$ °K are therefore not inconsistent with the estimated importance of the scattering mechanisms discussed in Sec. IV B for $T < 300$ °K. At 77 °K, the values of A cannot be interpreted by the Seitz theory. Although there is some indication of a decrease in K_+ with decreasing temperature in sample 96AMII, corresponding to a possible increase in $K_\tau = (\tau_\perp/\tau_\parallel)$ due to ionized-impurity scattering, the trend is obscured by effects which may be related to impurity conduction.

D. Band model

We have used hydrostatic pressure and transport measurements to demonstrate the inverting of the order of the Γ and L conduction bands in GaSb. Magnetoresistance measurements near room temperature establish that band conduction for $P > P_s$ takes place in the [111] valleys; for $K_\tau = 1$, the

mass anisotropy derived at room temperature is consistent with values previously inferred from measurements involving both Γ- and L-band conduction,[23] or interpolated from Ge data.[5]

The presence of Te states associated with the L minima has been established from the temperature dependence of the resistivity. These results confirm previous indications of the presence of such states from pressure measurements at fixed temperature. The concentration dependence of the activation energy for this impurity has been surveyed, and appears to be similar to the behavior observed for shallow donors in other semiconductors. Although the Te activation energy approaches zero with increasing concentration, there is no indication that the Fermi level lies in the L band in the highest-concentration samples available in the present study. Indeed, the results suggest that the initiation of L-band filling at $T = 0$ °K and $P > P_s$ probably requires $N_D - N_A \geq 7\times10^{18}$ cm^{-3}. Matsubara and Toyozawa[54] relate the Bohr radius of the donor electron in the hydrogenic model to the donor concentration n_{cb} at which the Fermi level should pass into the conduction band of the host lattice. Alexander and Holcomb[55] point out that in this case n_{cb} is a factor ~5 higher than the concentration estimated for delocalization of impurity states according to the Mott criterion.[41] In n-GaSb(Te), delocalization occurs at n ~6×10^{17} cm^{-3}, as stated previously. Our results therefore gave an experimental ratio of n_{cb}/n_c a factor 2 higher than predicted by Matsubara and Toyozawa.

We have detailed mobility behavior indicating that metallic-type impurity conduction becomes important at low temperatures in high-concentration samples. Previously, it had been assumed that at $P = 0$ and low temperatures, the populating of the L minima occurs for values of $N_D - N_A > N_c = 1.25\times10^{18}$ cm^{-3}.[13] This conjecture was based on the observation that at $P = 0$, the 4.2 °K transverse magnetoresistance is zero for $N < N_c$. According to the model, zero transverse magnetoresistance is expected in a spherical band when degenerate statistics apply. The presence of a second similar, but lower mobility band may be detected by the appearance of transverse magnetoresistance when the mobilities of the two bands are appreciably different. Thus the results suggested that for $N < N_c$, conduction takes place in the Γ minimum only; filling of the L band is initiated for $N > N_c$ leading to the rise in transverse magnetoresistance. Our present data indicates that this observation may be related to impurity conduction by carriers in the L band. In the earlier analysis,[13] a mobility ratio of $\mu_L/\mu_\Gamma = 0.06$ was obtained from a fit to the magnetoresistance data. We find for sample 80BIII, μ_H (4.2 °K, $P > P_s$)/μ_H (4.2 °K, $P = 0$) = 500/7830 = 0.064, consistent with the earlier result, but now interpreted in terms of impurity conduction rather than band conduction.

---

†Supported by the National Science Foundation (MRL Program No. GH33574A-1).

[1] R. T. Bate, J. Appl. Phys. 33, 26 (1962).
[2] H. Kaplan, J. Phys. Chem. Solids 24, 1593 (1963).
[3] G. A. Peterson, in *Proceedings of the Seventh International Conference on the Physics of Semiconductors, Paris*, 1964, edited by M. H. Hulin (Dunod, Paris, 1964), p. 771.
[4] T. Shimizu, Phys. Lett. 15, 297 (1965).
[5] B. B. Kosicki, Harvard University Technical Report No. HP-19, 1967 (unpublished); B. B. Kosicki and W. Paul, Phys. Rev. Lett. 17, 246 (1966).
[6] A. Sagar, Phys. Rev. 117, 93 (1960).
[7] D. G. Pitt, High Temp. High Pressure 1, 118 (1969).
[8] B. B. Kosicki, A. Jayaraman, and W. Paul, Phys. Rev. 172, 764 (1968).
[9] G. W. Ahlgren, W. M. Becker, and J. Stankiewicz, in *Proceedings of the Eleventh International Conference on the Physics of Semiconductors, Warsaw*, 1972 (Polish Scientific Publ., Warsaw, 1972), p. 438.
[10] J. Basinski, S. D. Rosenbaum, S. L. Basinski, and J. C. Woolley, J. Phys. C 6, 422 (1973).
[11] Ru-Yih Sun and W. M. Becker, Solid State Commun. 13, 1481 (1973).
[12] J. Stankiewicz, W. Giriat, and A. Bienenstock, Phys. Rev. B 4, 4465 (1972).
[13] W. M. Becker, A. K. Ramdas, and H. Y. Fan, J. Appl. Phys. 32, 2094 (1961).
[14] R. S. Allgaier, J. Appl. Phys. 36, 2429 (1965).
[15] T. O. Yep and W. M. Becker, Phys. Rev. 156, 939 (1967).
[16] N. T. Sherwood, Ph.D. thesis (Purdue University, 1970) (unpublished).
[17] A. K. Bhattacharjee and S. Rodriguez, Nuovo Cimento B 13, (1973).
[18] G. W. Ahlgren, Ph.D. thesis (Purdue University, 1972) (unpublished).
[19] J. S. Blakemore, *Semiconductor Statistics* (Pergamon, New York, 1962), p. 135.
[20] T. O. Yep and W. M. Becker, Phys. Rev. 144, 741 (1966).
[21] F. Seitz, Phys. Rev. 79, 372 (1950).
[22] H. Brooks, in *Advances in Electronics and Electron Physics*, edited by L. Marton (Academic, New York, 1955), Vol. 7, p. 85.
[23] H. Piller, Ref. 3, p. 297; C. Y. Liang, H. Piller, and D. L. Stierwalt, Appl. Phys. Lett. 12, 49 (1968).
[24] W. Kohn and J. M. Luttinger, Phys. Rev. 98, 915 (1955).
[25] G. L. Pearson and J. Bardeen, Phys. Rev. 75, 865 (1949).
[26] P. P. Debye and E. M. Conwell, Phys. Rev. 93, 693 (1954).
[27] J. M. Ziman, *Electrons and Phonons* (Oxford, U. P. London, 1962), p. 434.
[28] H. Ehrenreich, J. Phys. Chem. Solids 9, 129 (1959).
[29] H. B. Callen, Phys. Rev. 76, 1394 (1949).
[30] D. J. Howarth and E. H. Sondheimer, Proc. R. Soc.

A219, 53 (1953).
[31]D. J. Olechna and H. Ehrenreich, J. Phys. Chem. Solids 23, 1513 (1962).
[32]J. Bardeen and W. Shockley, Phys. Rev. 80, 72 (1950).
[33]F. J. Blatt, in *Solid State Physics*, edited by F. Seitz and D. Turnbull (Academic, New York, 1957), Vol. 4, p. 344.
[34]R. D. Baxter, F. J. Reid, and A. C. Beer, Phys. Rev. 162, 718 (1967).
[35]R. A. Smith, *Semiconductors* (Cambridge U. P., Cambridge, 1959), p. 151.
[36]P. Norton, T. Braggins, and H. Levinstein, Phys. Rev. B 8, 5632 (1973).
[37]C. Erginsoy, Phys. Rev. 79, 1013 (1950).
[38]R. P. Khosla, Phys. Rev. 183, 695 (1969).
[39]F. Martino, G. Lindell, K. F. Berggren, Phys. Rev. B 8, 6030 (1973).
[40]J. B. Krieger and M. Nightingale, Phys. Rev. B 4, 1266 (1971).
[41]N. F. Mott, Can. J. Phys. 34, 1356 (1956).
[42]H. Fritzsche, Phys. Rev. 125, 1552 (1962).
[43]M. Cuevas and H. Fritzsche, Phys. Rev. 137, A1847 (1965).
[44]M. Cuevas and H. Fritzsche, Phys. Rev. 139, A1628 (1965).
[45]J. B. Krieger, T. Meeks, and E. Esposito, Phys. Rev. B 3, 1262 (1971).
[46]J. B. Krieger, T. Meeks, and E. Esposito, Phys. Rev. B 5, 1499 (1972).
[47]J. B. Krieger and T. Meeks, Phys. Rev. B 8, 2780 (1973).
[48]M. Katz, Phys. Rev. 140, A1323 (1965).
[49]E. A. Davis and W. D. Compton, Phys. Rev. 140, A2183 (1965).
[50]E. Abeles and S. Meiboom Phys. Rev. 95, 31 (1954).
[51]M. Shibuya, Phys. Rev. 95, 1385 (1954).
[52]C. Herring and E. Vogt, Phys. Rev. 101, 944 (1956).
[53]A. C. Beer, in *Solid State Physics Supplement*, edited by F. Seitz and D. Turnbull (Academic, New York, 1963), Vol. 4, p. 230.
[54]T. Matsubara and Y. Toyozawa, Progr. Theor. Phys. 26, 739 (1961).
[55]M. N. Alexander and D. F. Holcomb, Rev. Mod. Phys. 40, 815 (1968).